College of Arts and Sciences

The Astronomical Journal, 133:214–219, 2007 January

DISCOVERY OF A GRAVITATIONALLY LENSED QUASAR FROM THE SLOAN DIGITAL SKY SURVEY: SDSS J133222.62+034739.9[1]

Tomoki Morokuma,[2] Naohisa Inada,[2,3] Masamune Oguri,[4,5] Shin-Ichi Ichikawa,[6] Yozo Kawano,[7] Kouichi Tokita,[2]
Issha Kayo,[7] Patrick B. Hall,[5,8] Christopher S. Kochanek,[9] Gordon T. Richards,[10,11]
Donald G. York,[12] and Donald P. Schneider[13]
Received 2006 August 11; accepted 2006 September 21

ABSTRACT

We report the discovery of the two-image gravitationally lensed quasar SDSS J133222.62+034739.9 (SDSS J1332+0347) with an image separation of $\Delta\theta = 1.14''$. This system consists of a source quasar at $z_s = 1.445$ and a lens galaxy at $z_l = 0.191$. The agreement of the luminosity, ellipticity, and position angle of the lens galaxy with those expected from a lens model confirms the lensing hypothesis.

Key words: gravitational lensing — quasars: individual (SDSS J133222.62+034739.9)

1. INTRODUCTION

Strong gravitational lensing is a powerful probe of the large-scale properties of the universe (Kochanek 2006). The well-known physics makes it straightforward to use lensing in cosmological estimates of the dark energy (Turner 1990; Fukugita et al. 1990) and the Hubble constant (Refsdal 1964). The gravitational lensing effect depends solely on the mass density of the field, and it is also an ideal tool for studies of dark matter in galaxies and clusters of galaxies (e.g., Oguri et al. 2004a). The Cosmic Lens All Sky Survey (CLASS; Myers et al. 2003; Browne et al. 2003), which was conducted in the radio band, is the largest current statistical sample of lensed compact sources. However, the CLASS has only 13 lensed radio sources in its well-defined statistical sample. Larger lens samples are critical to using lensed quasars for cosmological and astrophysical tests.

Optical surveys for lensed quasars are both complementary to radio surveys such as the CLASS and likely to produce larger lens samples, since only 1/10 of quasars are radio-loud (Ivezić et al. 2002). Our SDSS Quasar Lens Search (SQLS; Oguri et al. 2006) is based on the Sloan Digital Sky Survey (SDSS; York et al. 2000) and its catalog of roughly 100,000 spectroscopically confirmed quasars (e.g., Schneider et al. 2005). So far, the SQLS has succeeded in discovering 14 new lensed quasars (Inada et al. 2003a, 2003b, 2003c, 2005, 2006; Johnston et al. 2003; Morgan et al. 2003; Pindor et al. 2004, 2006; Oguri et al. 2004b, 2005; S. Burles et al. 2007, in preparation), as well as recovering many previously known lensed quasars (Walsh et al. 1979; Weymann et al. 1980; Surdej et al. 1987; Bade et al. 1997; Oscoz et al. 1997; Schechter et al. 1998; Morgan et al. 2001). Indeed, the number of SDSS-discovered lensed quasars is already a significant fraction of all known quasar lenses ($\sim$80).[14] The large number of lenses contained in the SQLS and its well-defined selection function mean that the lens catalog provided by the SQLS will be very useful for statistical studies of strong lensing (Oguri et al. 2006).

In this paper we report the discovery of a gravitationally lensed quasar, SDSS J133222.62+034739.9 (hereafter SDSS J1332+0347). The quasar was confirmed to be doubly imaged by a low-redshift early-type galaxy from observations using the Subaru 8.2 m telescope and the University of Hawaii 2.2 m (UH88) telescope. This paper is organized as follows: The SDSS data for SDSS J1332+0347, including its selection, are described in § 2. The follow-up images and spectra are shown in §§ 3 and 4, respectively. In § 5 we model the lens. Finally, we summarize our results in § 6. Throughout the paper we assume a cosmological model with matter density $\Omega_M = 0.27$, cosmological constant $\Omega_\Lambda = 0.73$, and Hubble constant $h = H_0/100$ km s^{-1} Mpc^{-1} = 0.7. Magnitudes are measured in the AB system.

2. SDSS DATA

The SDSS is a survey conducting both optical imaging and spectroscopy. It covers about 10,000 deg^2 of the sky, approximately centered on the north Galactic cap with the dedicated wide-field 2.5 m telescope (Gunn et al. 2006) at the Apache Point Observatory in New Mexico, USA. The five-broadband photometric data are taken in imaging surveys (Fukugita et al. 1996; Gunn et al. 1998; Lupton et al. 1999; Tucker et al. 2006) and are reduced automatically by a photometric pipeline (Lupton et al. 2001). From the magnitudes, colors, and morphologies of each object, quasar and galaxy candidates are selected as spectroscopic targets (Eisenstein et al. 2001; Richards et al. 2002; Strauss et al. 2002) and then assigned for spectroscopic observations by the tiling algorithm (Blanton et al. 2003). The spectra cover the wavelength range from 3800 to 9200 Å with a resolution of $R \sim 1800$. The astrometric accuracy is better than

[1] Based in part on data collected at Subaru telescope, which is operated by the National Astronomical Observatory of Japan.
[2] Institute of Astronomy, Faculty of Science, University of Tokyo, Mitaka, Tokyo, Japan.
[3] Japan Society for the Promotion of Science Research Fellow.
[4] Kavli Institute for Particle Astrophysics and Cosmology, Stanford University, Menlo Park, CA, USA.
[5] Princeton University Observatory, Princeton, NJ, USA.
[6] National Astronomical Observatory, Mitaka, Tokyo, Japan.
[7] Department of Physics and Astrophysics, Nagoya University, Chikusa-ku, Nagoya, Japan.
[8] Department of Physics and Astronomy, York University, Toronto, ON, Canada.
[9] Department of Astronomy, The Ohio State University, Columbus, OH, USA.
[10] Department of Physics and Astronomy, The Johns Hopkins University, Baltimore, MD, USA.
[11] Department of Physics, Drexel University, Philadelphia, PA, USA.
[12] Enrico Fermi Institute, The University of Chicago, Chicago, IL, USA.
[13] Department of Astronomy and Astrophysics, Pennsylvania State University, University Park, PA, USA.

[14] See the CASTLES Web site at http://cfa-www.harvard.edu/castles/.

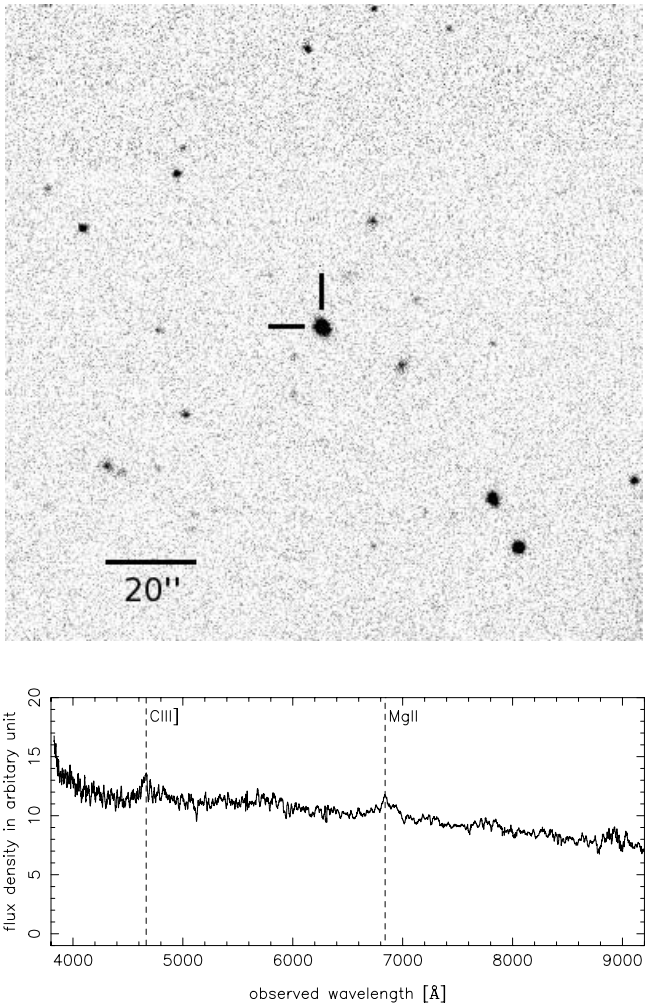

FIG. 1.—*Top*: Wide-field SDSS *i*-band image of SDSS J1332+0347. The pixel scale is 0.396″ pixel^{-1}. In the image, north is up and east is left. *Bottom*: SDSS spectrum of SDSS J1332+0347.

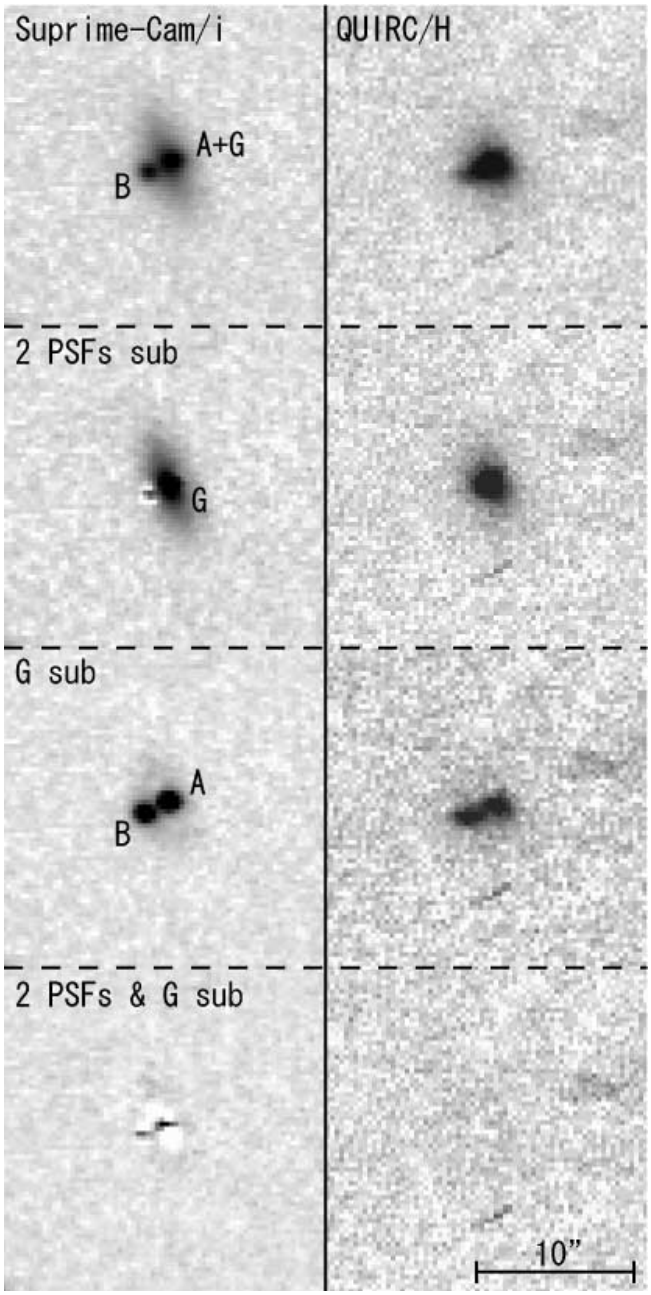

FIG. 2.—Follow-up images of SDSS J1332+0347. The optical *i*-band images taken with the Suprime-Cam on the Subaru telescope are shown in the left panels, while the near-infrared *H*-band images taken with QUIRC on the UH88 telescope are displayed in the right panels. The original images, images after subtracting the two PSF components, images after subtracting the galaxy model, and images after subtracting both the PSF and galaxy components are shown in the first, second, third, and fourth rows, respectively. In all panels, the box size is 20″, and north is up and east is left. The pixel scales are 0.202″ pixel^{-1} (Suprime-Cam) and 0.189″ pixel^{-1} (QUIRC), respectively.

$\sim$0.1″ rms (Pier et al. 2003), and the photometric zero-point errors are less than $\sim$0.03 mag over the entire survey area (Hogg et al. 2001; Smith et al. 2002; Ivezić et al. 2004). Most of the data have already become publicly available (Stoughton et al. 2002; Abazajian et al. 2003, 2004, 2005; Adelman-McCarthy et al. 2006).

SDSS J1332+0347 was selected as a lensed quasar candidate from the SDSS quasar sample using the same selection algorithm as described in Inada et al. (2003a). In this algorithm the morphological parameters of each quasar are used to select lensed quasar candidates. SDSS J1332+0347 was also selected by an improved algorithm (Oguri et al. 2006) whose selection function has been extensively tested, and it is in the well-defined source quasar sample of the SQLS for lensed quasar statistics.

Figure 1 shows the SDSS *i*-band image of the field under a seeing of 1.6″. The SDSS point-spread function (PSF) magnitudes

TABLE 1
SDSS J1332+0347: SDSS PHOTOMETRY AND REDSHIFT

u[a]	g[a]	r[a]	i[a]	z[a]	Redshift[b]
19.12 ± 0.03	18.61 ± 0.03	18.26 ± 0.02	17.95 ± 0.02	17.84 ± 0.02	1.438 ± 0.003

[a] PSF magnitudes from the SDSS imaging data.
[b] Quasar redshift from the SDSS spectrum.

TABLE 2
SDSS J1332+0347: Astrometry and Photometry

Object	x (arcsec)[a]	y (arcsec)[a]	i[b]	H[b]
A.....	0.000 ± 0.006	0.000 ± 0.006	19.28 ± 0.03	17.72 ± 0.17
B.....	−1.024 ± 0.006	−0.501 ± 0.006	19.66 ± 0.02	17.85 ± 0.05
G.....	−0.228 ± 0.013	−0.119 ± 0.013	18.64 ± 0.02	16.28 ± 0.04

Note.—All the values are the outputs of the GALFIT procedure for SDSS J1332+0347.
[a] The positive directions of x and y are west and north, respectively. The values are measured in the Subaru Suprime-Cam i-band image.
[b] The errors do not include the absolute calibration uncertainty.

and the quasar redshift are summarized in Table 1. The SDSS images indicate that the object is more extended than a single star, making it a good lens candidate and a target for higher angular resolution observations.

3. IMAGING OBSERVATIONS

We obtained a 90 s i-band image of SDSS J1332+0347 with the Suprime-Cam (Miyazaki et al. 2002) on the Subaru 8.2 m telescope at Mauna Kea in seeing of 0.5″ on 2003 May 28. The i-band image was reduced in a standard way for the Suprime-Cam data using the NEKO software (Yagi et al. 2002) and the SDFRED package (Ouchi et al. 2004). The absolute flux was calibrated using nearby stars in the SDSS catalogs. The small differences between the SDSS and Suprime-Cam i-band response functions are not important here. We also acquired a 720 s H-band image of this object with the Quick Infrared Camera (QUIRC) on the UH88 telescope in 0.8″ seeing on 2005 February 20. The H-band image was reduced in a standard

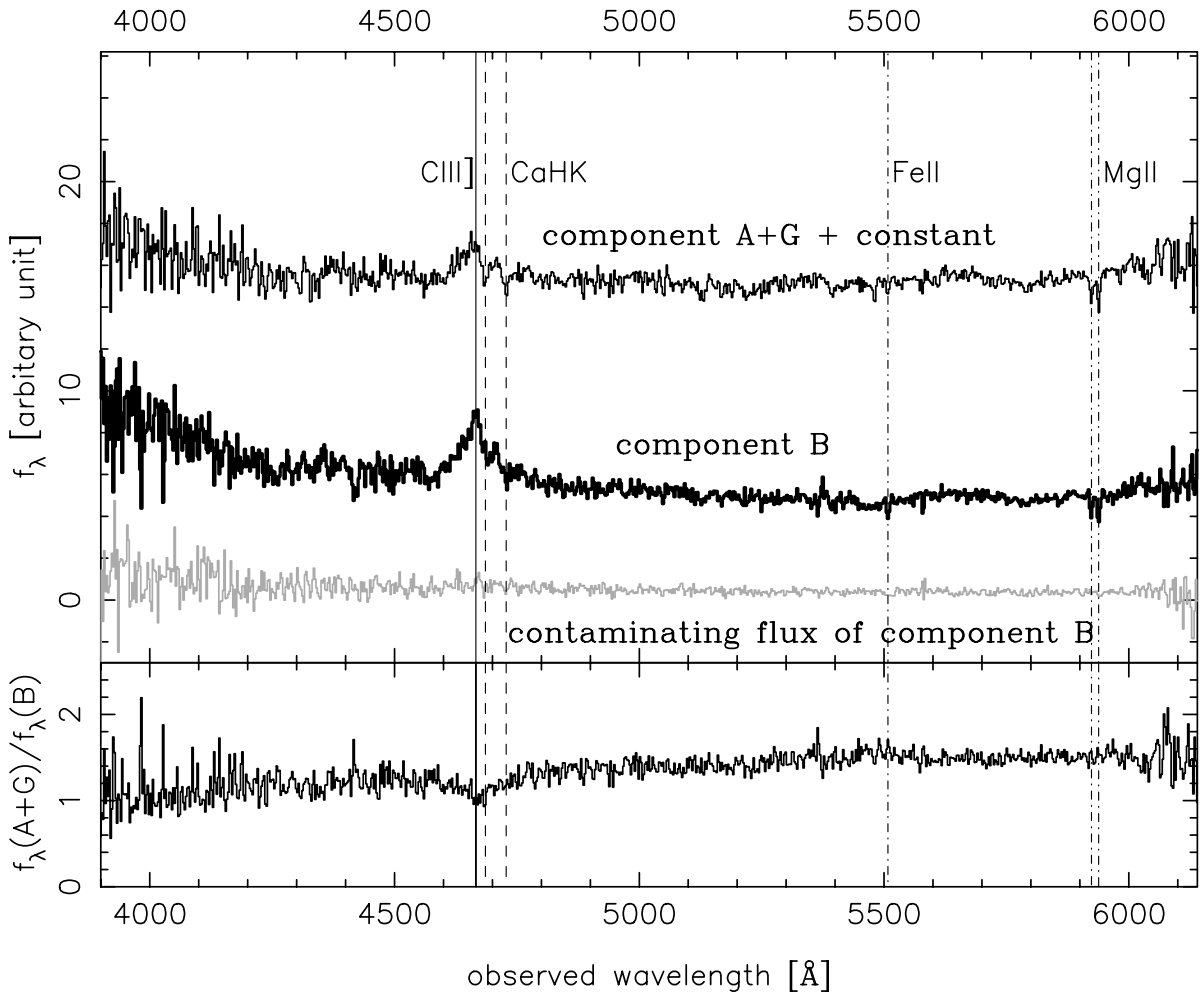

Fig. 3.—*Top*: Spectra ($R \sim 700$) of components A+G (*thin black solid line*) and B (*thick black solid line*) obtained with the Subaru FOCAS. The spectrum of component A+G is shifted by a constant to make it visible. A spectrum extracted at the same distance from component B as component A+G but in the opposite direction is also shown by the gray solid line. C III] emission lines (*vertical solid line*) in components A and B at $z = 1.445$, and Ca II H and K absorption lines (*vertical dashed line*) of galaxy G at $z = 0.191$, are detected. Fe II and Mg II absorption lines from an intervening system at $z = 1.119$ are also detected (*vertical dot-dashed line*). The Mg II absorption line doublet ratio of 1.0 is typical of such systems (e.g., Steidel & Sargent 1992). *Bottom*: Spectral flux ratio between components A+G and B.

TABLE 3
SDSS J1332+0347: Central Wavelengths of C III]

Object	λ_{obs}	z_{obs}	λ_{peak}	z_{peak}	λ_{mask}	z_{mask}
A+G.....	4653.49	1.4380	4661.11	1.4420	4666.23	1.4447
B.....	4663.26	1.4431	4666.08	1.4446	4666.25	1.4447

way using IRAF[15] and calibrated using the standard star FS 23 (Hawarden et al. 2001).

The *i* and *H* images are shown in Figure 2. Taking a closer look at the images, especially the *i*-band Suprime-Cam image, we see two compact sources bracketing an extended elliptical source. Indeed, models of the images using the public software GALFIT (Peng et al. 2002), consisting of two point sources and an extended object with a de Vaucouleurs profile between them, fit the data well. We used stars in the images as templates for the PSF in this procedure. We also show the observed galaxy after subtracting models for the two point sources, the observed stellar components after subtracting models for the galaxy, and the residuals after subtracting models for the point sources and the galaxy in the second, third, and fourth rows of Figure 2, respectively. We name the two stellar components A and B, where A is the brighter component that lies closer to the galaxy (separated by $\sim 0.26''$), component G. The separation of the two stellar components derived from the *i*-band image is $\Delta\theta = 1.14''$, and our relative astrometry is summarized in Table 2. The stellar components have similar colors of $i - H \sim 1.6$ and ~ 1.8 mag for A and B, respectively, while the galaxy G has a redder color of $i - H \sim 2.4$ mag. The photometry of the components is also summarized in Table 2. These astrometric and photometric properties are typical of known lensed quasar systems (e.g., Inada et al. 2006) and imply that both components A and B are lensed images of a quasar and that component G is a lens galaxy.

4. SPECTROSCOPIC OBSERVATIONS

We carried out a spectroscopic observation of SDSS J1332+0347 using the Faint Object Camera and Spectrograph (FOCAS; Kashikawa et al. 2002) installed on the Subaru 8.2 m telescope on 2003 June 20 with an exposure time of 900 s in $0.8''$ seeing. The observation was conducted in 2×2 on-chip binning mode, using a $0.6''$ width slit aligned along components A and B, with the grism 300B and the filter L600. This configuration provides a spectrum covering 3900–6000 Å with a spectral resolution of $R \sim 700$, a spectral dispersion of 2.7 Å pixel^{-1}, and a spatial pixel scale of $0.208''$. We used IRAF to analyze the spectra, extracting two traces corresponding to a blend of image A with the galaxy G and image B, respectively.

The two spectra are shown in Figure 3. We clearly see broad C III] emission lines redshifted to $z = 1.4$. On the red wings of the C III] emission lines, we also see an absorption doublet at 4686 and 4728 Å, which we interpret as Ca II H and K absorption lines redshifted to $z = 0.191$. These strong absorption lines significantly distort the emission lines. It would be helpful to have a cleaner emission line in order to determine the quasar redshifts more accurately, but the C III] emission lines are the only strong emission lines in the FOCAS spectra. We estimated the quasar redshifts using three approaches: (1) using the whole line profiles (λ_{obs}), (2) using only the line peaks (λ_{peak}), and (3) using the whole line profiles after masking and then interpolating through the absorption lines (λ_{mask}). The results, summarized in Table 3, confirm that the two quasars have the same redshifts. We adopt procedure 3 for our standard result of $z = 1.445$, as it is likely to be the most reliable. We also verified that the A+G spectrum has little contamination from quasar B by extracting a spectrum at the same distance from component B as component A+G but in the opposite direction. The spectrum, shown in Figure 3, has no significant emission, and we conclude that the C III] emission line in the A+G spectrum is due to component A. Furthermore, in the spectra of both components A+G and B, we can see Mg II $\lambda\lambda$2796, 2803 doublet absorption lines and a Fe II λ2600 absorption line from an intervening object at $z = 1.119$.

The spectral flux ratio between components A+G and B, displayed in Figure 3 (*bottom*), indicates that the combination of A+G is redder than component B. If we scale the spectrum of B by the *H*-band flux ratio of 1.127 between components A and B and subtract it from the spectrum A+G, then we obtain the residual spectrum shown in Figure 4. While the spectrum is noisy, especially around the C III] emission line and toward the blue wavelength region, the spectral energy distribution (SED) is consistent with a template spectrum of an elliptical galaxy (Kinney et al. 1996) at the redshift of the Ca II absorption feature, $z = 0.191$. Given the strength of the absorption, we conclude that the SEDs of components A and B are identical and that component G is an elliptical galaxy at $z = 0.191$.

5. LENS MODEL

We used the *lensmodel* package (Keeton 2001) to fit a mass model to the observations of SDSS J1332+0347, assuming that

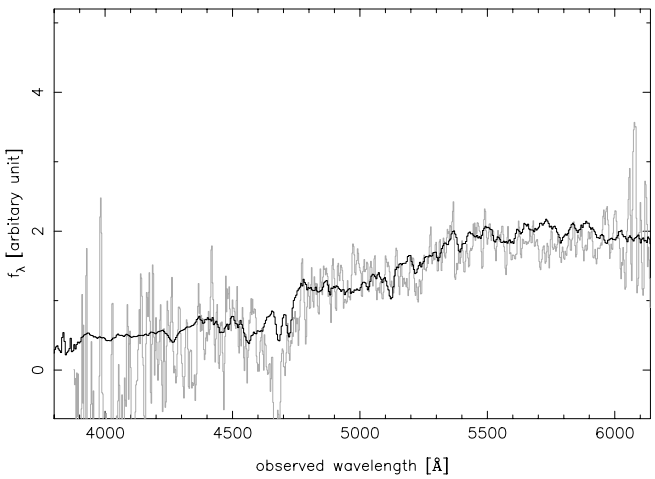

FIG. 4.—Spectrum of component G (*gray line*) obtained by subtracting a scaled (multiplied by 1.127) spectrum of component B from that of component A+G. The derived galaxy spectrum does not clearly show the Ca II H and K absorption lines but is consistent with a template spectrum of an elliptical galaxy (Kinney et al. 1996) at $z = 0.191$ (*black line*). This result indicates that components A and B have identical SEDs and redshifts.

[15] IRAF is the Image Reduction and Analysis Facility, a general-purpose software system for the reduction and analysis of astronomical data. IRAF is written and supported by the IRAF programming group at the National Optical Astronomy Observatory (NOAO) in Tucson, Arizona. NOAO is operated by the Association of Universities for Research in Astronomy, Inc., under cooperative agreement with the National Science Foundation.

TABLE 4
SDSS J1332+0347: Lens Model

Parameter	Value
Einstein radius	$R_{\rm E} = 0.465''$
Ellipticity	$e = 0.53 \pm 0.07$
Position angle[a]	$\theta_e = 25^\circ \pm 2^\circ$
Total magnification	$\mu_{\rm tot} = 4.1$
Time delay	$\Delta t = 6.7\ h^{-1}$ days

[a] Each position angle is measured east of north.

the object is indeed a lensed quasar system. We assume the standard singular isothermal ellipsoid model characterized by eight parameters: the Einstein radius $R_{\rm E}$, ellipticity e, position angle θ_e, position of the lensing galaxy, and position and flux of the source quasar. Since the number of observable constraints is also eight (the positions of A, B, and G and the fluxes of A and B), the number of degrees of freedom is 0. As expected, we were able to find a model that perfectly reproduces the observables, $\chi^2 \sim 0$. The results of the model are presented in Table 4. We note that the best-fit values for the ellipticity and the position angle, $e = 0.53 \pm 0.07$ and $\theta_e = 25^\circ \pm 2^\circ$, are in good agreement with those observed for the galaxy G (derived using GALFIT in the i-band image; see Fig. 2) of $e = 0.69$ and $\theta_e = 21^\circ$, respectively.

Einstein radii $R_{\rm E}$ are related to the velocity dispersions of lensing galaxies, so we can use the Faber-Jackson relation (Faber & Jackson 1976) to estimate the luminosity of the lens galaxy. From the best-fit value $R_{\rm E} = 0.465''$, we estimate that the apparent magnitude of the lens is $i = 18.8$, assuming the correlation of velocity dispersions and magnitudes of early-type galaxies derived by Bernardi et al. (2003). This is again in good agreement with the observed magnitude of the galaxy G, $i = 18.6$ (Table 2), implying that galaxy G is responsible for most of the lens potential.

6. CONCLUSIONS

We have presented extensive follow-up observations of SDSS J1332+0347 using the Subaru and UH88 telescopes. We found a bright galaxy (component G) between two stellar components (components A and B) with similar color in both the Subaru Suprime-Cam i-band and UH88 QUIRC H-band images. Although the C III] emission lines of the two stellar components are distorted by the Ca II H and K absorption lines from the bright galaxy at $z_l = 0.191$, we can still confirm that the two quasars are at the same redshift, $z_s = 1.445$. Subtraction of a scaled spectrum of component B from component A+G leaves a residual that is consistent with the spectrum of an elliptical galaxy redshifted to $z = 0.191$. The observed luminosity, ellipticity, and position angle of the bright galaxy are in good agreement with those expected from a standard lens model. All these results lead us to the conclusion that SDSS J1332+0347 is indeed a lensed quasar system, where a source quasar at $z_s = 1.445$ is lensed by a bright lens galaxy at $z_l = 0.191$, resulting in an image separation of $\Delta\theta = 1.14''$. One peculiar characteristic of the lens is that the brighter component A is closer to the lens galaxy than the fainter component B. We have no difficulty reproducing the flux ratio, and note that such *inverted* flux ratios were also observed and easily modeled in the two-image lens HE 1104−1805 (Wisotzki et al. 1993). This discovery adds another object to the complete sample of SDSS lensed quasars that can be used to estimate the cosmological model. The brightness of the lens galaxy also makes it a good candidate for dynamical observations; higher resolution imaging would allow us to determine more accurately the brightness of the components in this lens system, and spectroscopic observations with better signal-to-noise ratios would also allow us to study the interstellar medium in the lens galaxy in detail.

N. I. is supported by the Japan Society for the Promotion of Science (JSPS) through a JSPS Research Fellowship for Young Scientists. This paper is based in part on data collected at the Subaru telescope, which is operated by the National Astronomical Observatory of Japan (NAOJ). Use of the University of Hawaii 2.2 m telescope for observations is supported by the NAOJ. I. K. acknowledges support from a Ministry of Education, Culture, Sports, Science, and Technology Grant-in-Aid for Encouragement of Young Scientists (17740139). This work was supported in part by Department of Energy contract DE-AC02-76SF00515.

Funding for the SDSS and SDSS-II has been provided by the Alfred P. Sloan Foundation, the Participating Institutions, the National Science Foundation, the US Department of Energy, the National Aeronautics and Space Administration, the Japanese Monbukagakusho, the Max Planck Society, and the Higher Education Funding Council for England. The SDSS Web site is at http://www.sdss.org.

The SDSS is managed by the Astrophysical Research Consortium for the Participating Institutions. The Participating Institutions are the American Museum of Natural History, the Astrophysical Institute Potsdam, the University of Basel, Cambridge University, Case Western Reserve University, the University of Chicago, Drexel University, Fermilab, the Institute for Advanced Study, the Japan Participation Group, the Johns Hopkins University, the Joint Institute for Nuclear Astrophysics, the Kavli Institute for Particle Astrophysics and Cosmology, the Korean Scientist Group, the Chinese Academy of Sciences, Los Alamos National Laboratory, the Max Planck Institute for Astronomy, the Max Planck Institute for Astrophysics, New Mexico State University, the Ohio State University, the University of Pittsburgh, the University of Portsmouth, Princeton University, the United States Naval Observatory, and the University of Washington.

REFERENCES

Abazajian, K., et al. 2003, AJ, 126, 2081
———. 2004, AJ, 128, 502
———. 2005, AJ, 129, 1755
Adelman-McCarthy, J. K., et al. 2006, ApJS, 162, 38
Bade, N., Siebert, J., Lopez, S., Voges, W., & Reimers, D. 1997, A&A, 317, L13
Bernardi, M., et al. 2003, AJ, 125, 1849
Blanton, M. R., Lin, H., Lupton, R. H., Maley, F. M., Young, N., Zehavi, I., & Loveday, J. 2003, AJ, 125, 2276
Browne, I. W. A., et al. 2003, MNRAS, 341, 13
Eisenstein, D. J., et al. 2001, AJ, 122, 2267
Faber, S. M., & Jackson, R. E. 1976, ApJ, 204, 668
Fukugita, M., Futamase, T., & Kasai, M. 1990, MNRAS, 246, 24P
Fukugita, M., Ichikawa, T., Gunn, J. E., Doi, M., Shimasaku, K., & Schneider, D. P. 1996, AJ, 111, 1748
Gunn, J. E., et al. 1998, AJ, 116, 3040
———. 2006, AJ, 131, 2332
Hawarden, T. G., Leggett, S. K., Letawsky, M. B., Ballantyne, D. R., & Casali, M. M. 2001, MNRAS, 325, 563
Hogg, D. W., Finkbeiner, D. P., Schlegel, D. J., & Gunn, J. E. 2001, AJ, 122, 2129
Inada, N., et al. 2003a, AJ, 126, 666
———. 2003b, AJ, submitted
———. 2003c, Nature, 426, 810
———. 2005, AJ, 130, 1967
———. 2006, AJ, 131, 1934

Ivezić, Ž., et al. 2002, AJ, 124, 2364
———. 2004, Astron. Nachr., 325, 583
Johnston, D. E., et al. 2003, AJ, 126, 2281
Kashikawa, N., et al. 2002, PASJ, 54, 819
Keeton, C. R. 2001, ApJ, submitted (astro-ph/0102340)
Kinney, A. L., et al. 1996, ApJ, 467, 38
Kochanek, C. S. 2006, in Gravitational Lensing: Strong, Weak, and Micro, ed. G. Meylan, P. North, & P. Jetzer (Berlin: Springer), 91
Lupton, R., Gunn, J. E., Ivezić, Z., Knapp, G. R., Kent, S., & Yasuda, N. 2001, in ASP Conf. Ser. 238, Astronomical Data Analysis Software and Systems X, ed. F. R. Harnden, Jr., F. A. Primini, & H. E. Payne (San Francisco: ASP), 269
Lupton, R. H., Gunn, J. E., & Szalay, A. S. 1999, AJ, 118, 1406
Miyazaki, S., et al. 2002, PASJ, 54, 833
Morgan, N. D., Becker, R. H., Gregg, M. D., Schechter, P. L., & White, R. L. 2001, AJ, 121, 611
Morgan, N. D., Snyder, J. A., & Reens, L. H. 2003, AJ, 126, 2145
Myers, S. T., et al. 2003, MNRAS, 341, 1
Oguri, M., et al. 2004a, ApJ, 605, 78
———. 2004b, PASJ, 56, 399
———. 2005, ApJ, 622, 106
———. 2006, AJ, 132, 999
Oscoz, A., Serra-Ricart, M., Mediavilla, E., Buitrago, J., & Goicoechea, L. J. 1997, ApJ, 491, L7
Ouchi, M., et al. 2004, ApJ, 611, 660
Peng, C. Y., Ho, L. C., Impey, C. D., & Rix, H.-W. 2002, AJ, 124, 266
Pier, J. R., Munn, J. A., Hindsley, R. B., Hennessy, G. S., Kent, S. M., Lupton, R. H., & Ivezić, Ź. 2003, AJ, 125, 1559
Pindor, B., et al. 2004, AJ, 127, 1318
———. 2006, AJ, 131, 41
Refsdal, S. 1964, MNRAS, 128, 307
Richards, G. T., et al. 2002, AJ, 123, 2945
Schechter, P. L., Gregg, M. D., Becker, R. H., Helfand, D. J., & White, R. L. 1998, AJ, 115, 1371
Schneider, D. P., et al. 2005, AJ, 130, 367
Smith, A., et al. 2002, AJ, 123, 2121
Steidel, C. C., & Sargent, W. L. W. 1992, ApJS, 80, 1
Stoughton, C., et al. 2002, AJ, 123, 485
Strauss, M. A., et al. 2002, AJ, 124, 1810
Surdej, J., Swings, J.-P., Magain, P., Courvoisier, T. J.-L., & Borgeest, U. 1987, Nature, 329, 695
Tucker, D. L., et al. 2006, Astron. Nachr., 327, 821
Turner, E. L. 1990, ApJ, 365, L43
Walsh, D., Carswell, R. F., & Weymann, R. J. 1979, Nature, 279, 381
Weymann, R. J., et al. 1980, Nature, 285, 641
Wisotzki, L., Köhler, R., Kayser, R., & Reimers, D. 1993, A&A, 278, L15
Yagi, M., et al. 2002, AJ, 123, 66
York, D. G., et al. 2000, AJ, 120, 1579